

LETTERS

A distinct bosonic mode in an electron-doped high-transition-temperature superconductor

F. C. Niestemski¹, S. Kunwar¹, S. Zhou¹, Shiliang Li², H. Ding¹, Ziqiang Wang¹, Pengcheng Dai^{2,3} & V. Madhavan¹

Despite recent advances in understanding high-transition-temperature (high- T_c) superconductors, there is no consensus on the origin of the superconducting ‘glue’: that is, the mediator that binds electrons into superconducting pairs. The main contenders are lattice vibrations^{1,2} (phonons) and spin-excitations^{3,4}, with the additional possibility of pairing without mediators⁵. In conventional superconductors, phonon-mediated pairing was unequivocally established by data from tunnelling experiments⁶. Proponents of phonons as the high- T_c glue were therefore encouraged by the recent scanning tunnelling microscopy experiments on hole-doped $\text{Bi}_2\text{Sr}_2\text{CaCu}_2\text{O}_{8-\delta}$ (BSCCO) that reveal an oxygen lattice vibrational mode whose energy is anticorrelated with the superconducting gap energy scale⁷. Here we report high-resolution scanning tunnelling microscopy measurements of the electron-doped high- T_c superconductor $\text{Pr}_{0.88}\text{LaCe}_{0.12}\text{CuO}_4$ (PLCCO) ($T_c = 24$ K) that reveal a bosonic excitation (mode) at energies of 10.5 ± 2.5 meV. This energy is consistent with both spin-excitations in PLCCO measured by inelastic neutron scattering (resonance mode)⁸ and a low-energy acoustic phonon mode⁹, but differs substantially from the oxygen vibrational mode identified in BSCCO. Our analysis of the variation of the local mode energy and intensity with the local gap energy scale indicates an electronic origin of the mode consistent with spin-excitations rather than phonons.

Electron- and hole-doped high- T_c superconductors share identical CuO_2 planes where superconductivity originates. Compared with their hole-doped counterparts, the electron-doped copper oxide superconductors represent a largely unexplored territory for scanning tunnelling microscopy (STM) studies where the lack of high-quality samples has posed a tremendous barrier to obtaining high-quality data comparable to that on BSCCO. We have obtained reproducible STM data on nearly optimally doped PLCCO ($T_c = 24$ K) used in recent neutron scattering⁸ and angle-resolved photoemission spectroscopy (ARPES) experiments¹⁰. Figure 1 shows selected STM spectra illustrating the most prominent features in the density of states (DOS): the superconducting gap with coherence peaks, and the step or peak features outside the gap. In addition to these, an obvious feature of the tunnelling spectra is the presence of an almost linear, V-shaped background (Fig. 1b, see also Supplementary Fig. 2) which persists above T_c (Fig. 2d). A similar background was observed in previous STM data on the electron-doped superconductor $\text{Nd}_{2-x}\text{Ce}_x\text{CuO}_4$ (NCCO)¹¹. There are several different conjectures for a linear background in the DOS, ranging from momentum-dependent tunnelling matrix element effects in a marginal Fermi liquid¹² to inelastic tunnelling from a continuum of states¹³. Once this background is divided out, however, the muted spectral features (including the formerly suppressed coherence peak heights) come to the forefront as shown in Fig. 1c and d. To make

sure that the observed gap is associated with the superconducting gap, we have performed spectroscopy at various temperatures up to 32 K (above T_c) (Fig. 2d) and find that the gap does indeed disappear above T_c . We thus identify the peak-to-peak distance in the local density of states at 5.5 K with twice the local energy gap for superconducting quasiparticles (2Δ).

Although there have been no prior STM studies on PLCCO, ARPES studies¹⁴ point towards a non-monotonic d -wave gap with a maximum around 5.5 meV. Point contact tunnelling¹⁵ observes a zero temperature gap ($\Delta(0)$) of 3.5 meV with a ratio $2\Delta(0)/k_B T_c = 3.5 \pm 0.3$ consistent with weak-coupling BCS. Previous STM data obtained on NCCO¹¹ showed gaps of 3.5 to 5 meV with no obvious coherence peaks. Given the highly inhomogeneous nature of doped layered oxides, spatially resolved STM is a useful key to providing the local energy scales and spatial distribution of the superconducting gap. Statistics of the gap magnitude and its spatial variation were obtained through thousands of spectra (dI/dV mapping) in various regions of the sample (Fig. 2a and c). Although most maps (9 out of 13) reveal average gaps in the range of 6.5–7.0 meV, the average gap (over all measured maps) is 7.2 ± 1.2 meV (Fig. 2c). Approximating $\Delta(0)$ as 7.2 meV allows us to obtain a rough estimate for the ratio $2\Delta/k_B T_c \approx 7.5$, putting the electron-doped superconductors in the strong coupling regime, thereby suggesting a greater overlap between the fundamental physics of the electron- and hole-doped materials than previously shown.

We now turn to important features in the local density of states at energies greater than Δ . A step-like feature in the DOS (which results in a peak in the second derivative of the tunnel current d^2I/dV^2) is normally interpreted as the signature of a bosonic excitation in the system. STM data on bosonic excitations and the strengths of their coupling to the electrons could potentially provide critical information on viable candidates for the pairing mode. Shown in Fig. 3a is a typical dI/dV spectrum obtained on these samples. The derivative of the spectrum (Fig. 3b) reveals peaks at distinct energies marked E_1 and E_2 . In the superconducting state, a bosonic excitation appears in STM spectra at an energy offset by the gap, that is, $E = \Omega + \Delta$ where E is the energy of the feature in the spectrum and Ω is the mode energy. Although the line-shape of the feature could be influenced by the details of the process, both inelastic tunnelling effects¹⁶ and electron self-energy effects⁶ from a strongly coupled bosonic mode are expected at energies offset by the gap. This allows us conveniently to extract the mode energies for this spectrum ($\Omega_{1,2} = E_{1,2} - 7.0$ meV) resulting in 10.7 meV and 21.7 meV respectively. Because spectral features at multiples of Ω_1 could arise from multi-boson excitations, we find that $\Omega_{1,2}$ are amenable to interpretation as multiples of the same mode Ω_1 at 10.85 ± 0.15 meV.

To determine the statistical significance of the observation of this bosonic mode, we obtained high-resolution dI/dV maps over many

¹Department of Physics, Boston College, Chestnut Hill, Massachusetts 02467, USA. ²Department of Physics and Astronomy, The University of Tennessee, Knoxville, Tennessee 37996-1200, USA. ³Neutron Scattering Sciences Division, Oak Ridge National Laboratory, Oak Ridge, Tennessee 37831-6393, USA.

regions of the samples and analysed them to extract Δ and E locally. Data from one such map are shown in Fig. 3c. The observation of multiples of Ω_1 allows us to extract Ω_1 in two different ways for each spectrum: $\Omega_1 = E_1 - \Delta$ and $\Omega_1^* = E_2 - E_1$. These are independent observables whose histograms are plotted in Fig. 3d. As can be seen, the two histograms overlap strongly. We thus conclude that the identification of Ω_2 as $2\Omega_1$ bears significant statistical weight, which further supports the identification of these features outside the superconducting gap as originating from bosonic excitations in PLCCO. Using the data from eight dI/dV maps (Fig. 3e), we obtain an average mode energy of $\Omega_{1\text{av}} = 10.5 \pm 2.5$ meV. Both the intensity of Ω_1 and the observation of the second harmonic ($2\Omega_1$) of the mode indicate a relatively strong electron-mode coupling. From these spatially resolved spectra, we can also calculate the correlation

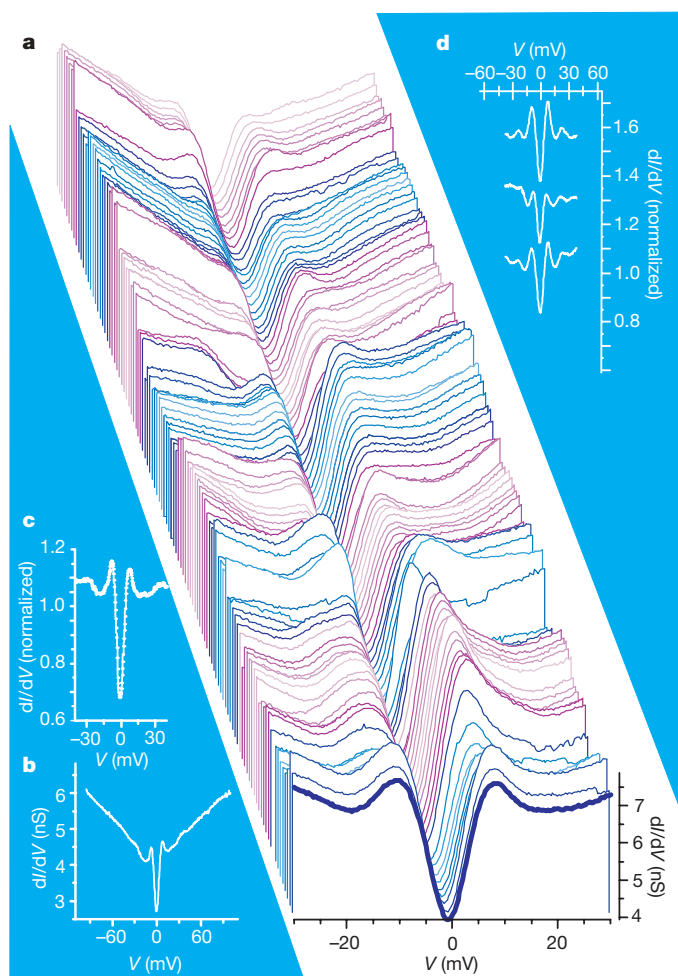


Figure 1 | Prominent low energy spectral features on PLCCO at a temperature of 5.5 K. **a**, A 200-Å section of a 512-Å linecut (a sequence of dI/dV spectra obtained along a spatial line) showing the variations in coherence peak heights and gap magnitude (Δ), defined as half the energy separation between the coherence peaks. The spectra have been offset for clarity. The gap magnitude in this linecut varies from 5 meV to 8 meV. For all spectra, V refers to sample voltage. The spectra were obtained with a junction resistance of 120 M Ω . **b**, A representative ± 100 -mV range (dI/dV) spectrum (200 M Ω junction resistance) illustrating the dominating V-shaped background. **c**, The linecut reveals spectra that vary from ones with sharp coherence peaks to pseudogap-like spectra without coherence peaks, but most spectra reveal coherence peaks of varying magnitudes once the dominating V-shaped linear background is divided out. This is illustrated by the spectrum shown here, which is the spectrum in **b** after a linear V-shaped division. **d**, More examples of dI/dV spectra demonstrating the clearly resolved coherence peaks and modes resulting from a V-shaped division. These spectra were obtained with 200 M Ω junction resistance.

between the local mode $\Omega(r)$ and the gap $\Delta(r)$. We find that $\Omega(r)$ is anticorrelated with the local gap magnitude $\Delta(r)$ as visible in Fig. 4a. The correlation function obtained between the two is fairly short-ranged, with a normalized on-site ($r = 0$) value close to -0.4 , comparable to that found⁷ in BSCCO. This anticorrelation is the first indication that this signal arises from an intrinsic excitation rather than an extrinsic inelastic excitation outside the superconducting planes.

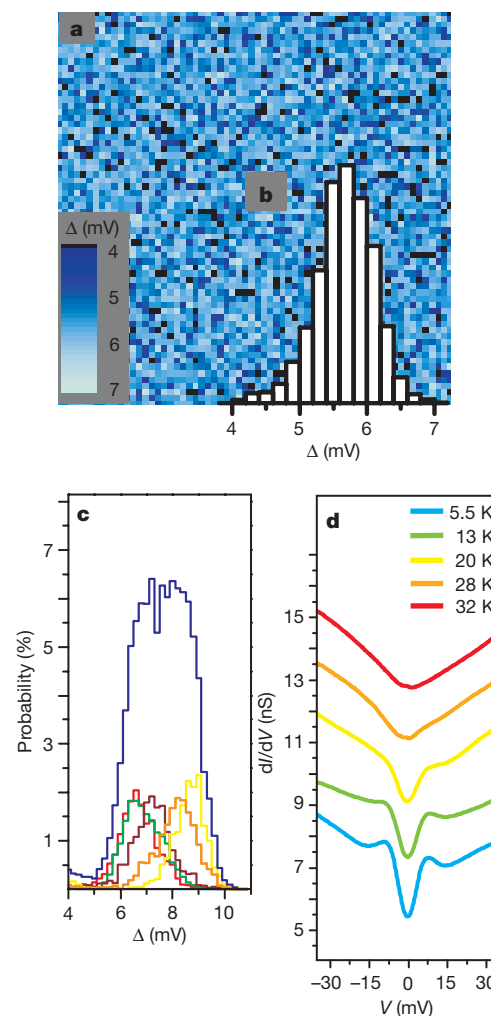


Figure 2 | Gap distribution, statistics and temperature dependence. **a**, A 64×64 pixel gap map taken on an area of $256 \text{ \AA} \times 256 \text{ \AA}$ at 5.5 K with a junction resistance of 500 M Ω . The corresponding topographic image reveals no atomic-scale corrugations, as is the common feature of STM images in the superconducting regions of PLCCO (see Supplementary Information), and has therefore been omitted. The patch size in these samples (defined as the area where the gap variation is in the range ± 0.5 meV) ranges from 30 Å to 100 Å or more. **b**, The gap distribution of the map in **a**. The average gap in this region is 6.7 ± 1.0 meV. This gap variation is much smaller than that observed in hole-doped BSCCO on a similar-sized region. **c**, Multiple histograms showing gap distributions in different regions of the sample. Our STM's coarse x - y motion capabilities (± 0.5 mm maximum) allow us to collect data in regions separated by larger length scales. The mean gap (for the regions represented here) ranges from 6.7 meV to 8.5 meV with a standard deviation ranging from 0.5 meV to 1 meV. Given these statistics, we conclude that gap variations in PLCCO occur on longer length scales than in BSCCO. The sum of these histograms is shown in blue. The average gap over all 13 maps that we obtained is 7.2 ± 1.2 meV. **d**, Temperature evolution of spatially averaged spectra. The spectra have been offset along the vertical axis for clarity. A 256-Å linecut (junction resistance of 120 M Ω) was averaged at each temperature shown, from 5.5 K to 32 K. By 28 K, the gap and coherence peaks have disappeared, but the V-shaped overall background remains.

Having established the mode energy and statistics, and its correlation to the local gap, we now discuss the nature of this excitation. Indeed, the measured mode energy of 10.5 ± 2.5 meV suggests an immediate connection to the 11-meV magnetic resonance mode discovered recently in PLCCO (ref. 8) and NCCO (ref. 17) at $Q = (\frac{1}{2}, \frac{1}{2}, 0)$ by inelastic neutron scattering. The neutron resonance mode, or more precisely its precursor above T_c , has been suggested as a possible pairing glue for the high- T_c copper oxides. Theoretically, bosonic modes originating from spin-excitations can be observed by STM provided there is sufficient coupling between the charge and spin degrees of freedom¹⁸. Magnetoresistance measurements on underdoped non-superconducting $\text{Pr}_{1.3-x}\text{La}_{0.7}\text{Ce}_x\text{CuO}_{4-\delta}$ have provided evidence for strong spin-charge coupling in these materials¹⁹. It is thus possible that the magnetic resonance mode observed by neutron scattering is related to the observed bosonic mode in the STM signal in PLCCO.

Although magnetic excitations fit the energy scale of our data, another possibility is that the mode originates from in-plane (CuO_2 plane) phonons, like the B_{1g} mode attributed to the STM feature in BSCCO. Compared with BSCCO, however, the energy

scale of our mode (10.5 ± 2.5 meV) is much lower. In the hole-doped superconductors a few phonon branches do exist at these low energies^{20,21} and the important question is whether there are candidate phonons at these low energies in PLCCO. As it turns out, many of the in-plane phonons in closely related materials, including the B_{1g} mode, have energies higher than 20 meV (refs 22–24) and can therefore be ruled out. Acoustic phonons are viable candidates for this mode provided that the phonon dispersion results in a sharp DOS feature at this energy scale. Such phonons with a DOS peak at or close to 11 meV have indeed been found^{9,25} in NCCO. Expanding the search to in-plane phonons at nearby energies reveals an E_u oxygen mode²³ and an oxygen rotation mode²² at energies greater than 15 meV (15 meV is the lowest energy in the dispersion). We thus conclude that whereas the energy scale of the observed mode clearly rules out the B_{1g} oxygen phonons, at least one in-plane phonon (acoustic) mode does exist at nearby energies.

Apart from these in-plane phonons, the STM mode might arise from inelastic co-tunnelling processes²⁶ involving an excitation of a local vibrational mode in the intervening layers between the tip and the superconducting plane ('barrier' mode). Such 'out-of-plane'

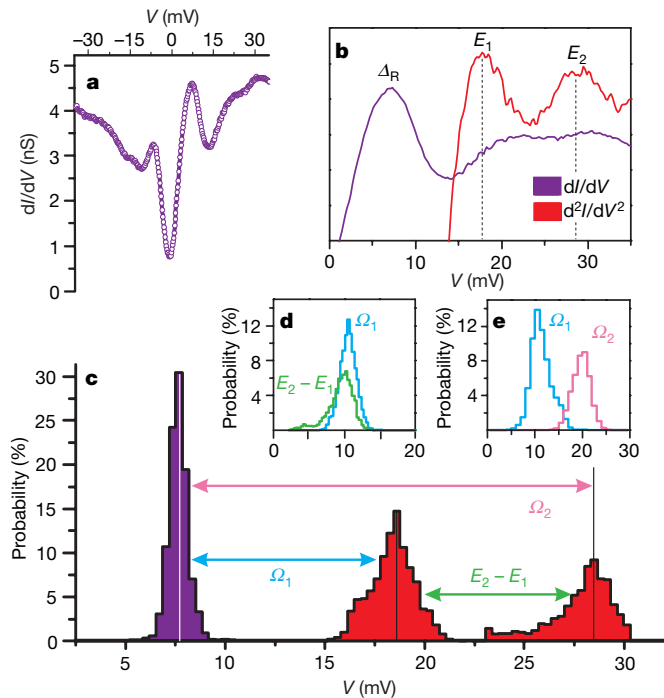


Figure 3 | Statistics of the mode observed as peaks in d^2I/dV^2 . **a**, A typical dI/dV spectrum taken at 5.5 K with a junction resistance of 200 M Ω demonstrating the appearance of the modes. **b**, The same spectrum from **a** (purple) as well as its derivative, d^2I/dV^2 (red). The linear V-shaped background has been divided out for clarity and the spectra are now shown only for energies greater than the Fermi energy (E_F). The peak in dI/dV (at 7.0 meV) is the coherence peak, labelled as Δ_R . The peaks in d^2I/dV^2 are labelled as E_1 and E_2 respectively. **c**, A histogram of the occurrences of Δ_R (purple) and the energies E_1 and E_2 (red) for a map of dI/dV on a $64 \text{ \AA} \times 64 \text{ \AA}$ area of the sample. We calculate the average gap (Δ_{av}) in this region to be 7.7 ± 0.5 meV, and the average peaks to be $E_{1av} = 18.5 \pm 1.5$ meV and $E_{2av} \approx 28$ meV (our cut-off at 30 meV for this analysis prevents us from obtaining full statistics for E_2). **d**, Following convention in superconducting systems, the mode energy will be symbolized by Ω ($\Omega_i = E_i - \Delta$). The mode energy is calculated in two ways for each spectrum in the map: $E_1 - \Delta_R$ (blue) with a mean of 10.7 ± 1 meV and $E_2 - E_1$ (green) with a mean of 10 ± 1.7 meV. These are two independent variables and the remarkable overlap between these histograms lends weight to their identification as multiples of the same mode. **e**, Histogram of the mode energies Ω_1 (blue) and Ω_2 (pink) summed for eight maps in different areas of the sample with gaps ranging from 6.5 meV to 8.5 meV. The mode energies were extracted from above and below E_F . From these data, we obtain the average mode energy $\Omega_{1av} = 10.5 \pm 2.5$ meV.

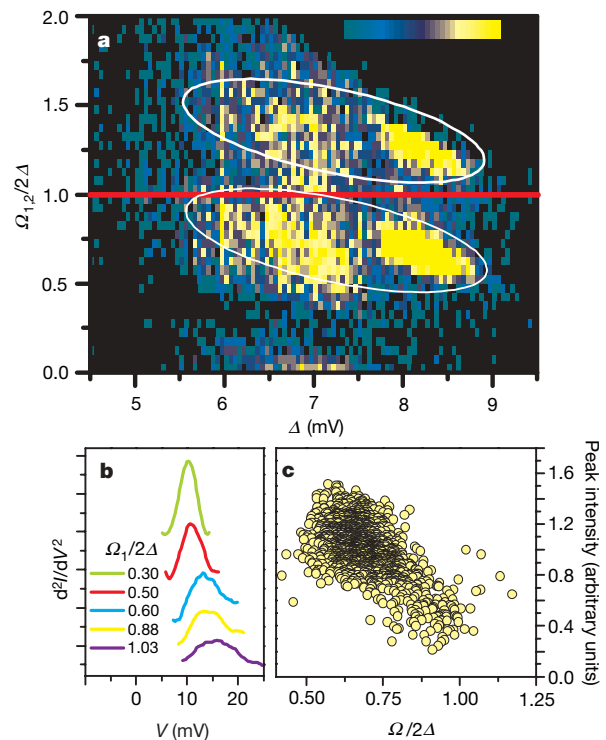


Figure 4 | Variation of local mode energy and intensity with the local gap energy scale. **a**, Log intensity (two-dimensional histogram; blue to yellow shows minimum to maximum) of the occurrences of Ω_1 and Ω_2 plotted as a local ratio $\Omega(r)/2\Delta(r)$ against $\Delta(r)$, clearly revealing the anticorrelation between Ω and Δ . Also note that $\Omega_1(r)/2\Delta(r)$ remains below 1 for a statistically significant part of the data (whereas $\Omega_2(r)/2\Delta(r)$ remains below 2). This demonstrates the sensitivity of the mode to the energy scale 2Δ , which is also borne out by the intensity analysis in **b** and **c**. This plot includes data from three maps obtained in regions of the sample with different average gap values. **b**, Examples of d^2I/dV^2 spectra (from one map) for different ratios of $\Omega_1/2\Delta$ from 0.3 to 1.03. The intensity of the mode (defined as the height of the peak in d^2I/dV^2 spectra) decreases and the mode gets wider in energy as Ω_1 approaches 2Δ . Although both Ω and Δ can vary from spectrum to spectrum, it is the local ratio of $\Omega(r)$ to $2\Delta(r)$ that determines the intensity of the mode. This is consistent with increased damping of the mode associated with the onset of the continuum of excitations at $2\Delta(r)$. **c**, A plot of the mode intensity (reiterating the same behaviour as in **b**) now for all the measured bosonic modes in a single map. Similar intensity drops with the ratio $\Omega_1/2\Delta$ were observed for maps in different regions with average gaps ranging from 6.5 meV to 8.5 meV.

phonons associated with the apical oxygen have been postulated as an alternative explanation for the BSCCO data¹⁶. Although barrier modes in PLCCO might originate from Pr/La/Ce vibrational excitations in the layers adjacent to the CuO₂ planes, it is not obvious how such modes would lead to our observed correlation between $\Omega(r)$ and $\Delta(r)$. Indeed, based on the idea that this correlation is significant, one recent analysis of the BSCCO STM data²⁷ postulates two coexisting bosonic modes, only one of which is sensitive to the superconducting gap and can be considered as a signature of the neutron resonance mode in BSCCO.

To bring more insight into the issue of electronic versus lattice-vibrational sources of this mode, we further explore its connection to the superconductivity energy gap. The local nature of STM spectroscopy makes it possible to study the relationship between the spectral properties of the local mode, and the energy scale for the onset of particle-hole excitations ($2\Delta(r)$). Figure 4a is a scatter plot showing the occurrences of the two modes Ω_1 and Ω_2 at a given Δ for three typical regions of different average gap sizes. It is clearly visible in the plot that the ratio $\Omega_1/2\Delta$ lies below 1 for a statistically significant fraction of the observed modes (and that $\Omega_2/2\Delta$ is capped by 2, consistent with the interpretation of Ω_2 as $2\Omega_1$). In Fig. 4b, we present the spectral lines of d^2I/dV^2 near the mode energy for several representative cases with different $\Omega_1/2\Delta$ ratios. Remarkably, the line-shape evolves from a sharp, symmetric feature resembling a resonance peak at low $\Omega_1/2\Delta$ to being broad and asymmetric (like an overdamped mode) as $\Omega_1/2\Delta$ approaches and exceeds one. As shown in Fig. 4c, a clear anticorrelation between the sharpness of the mode and $\Omega_1/2\Delta$ is observed, providing statistical significance for the line-shape analysis in Fig. 4b. These findings unequivocally demonstrate the intimate connection between the bosonic mode and the quasiparticle excitations across the superconducting energy gap. We note that although our analysis of the low-temperature STM data argues against the barrier modes, measurements of the normal-state ($T > T_c$) DOS will provide further, more direct data for the influence of the inelastic barrier co-tunnelling processes on the local tunnelling spectroscopy²⁸.

The overall picture that finally emerges from our STM studies on PLCCO is the observation of a collective mode in the electronic excitations of the system at 10.5 ± 2.5 meV. Although we cannot rule out low-energy phonons, this mode is fully consistent with the neutron spin resonance mode, and strongly coupled to the superconducting order parameter, making it a compelling candidate boson in the model based on the Eliashberg²⁹ framework, where exchanging associated electronic (spin or charge) excitations serves as the unconventional pairing mechanism in these materials.

Received 3 June; accepted 18 October 2007.

- McQueeney, R. J. *et al.* Anomalous dispersion of LO phonons in La_{1.85}Sr_{0.15}CuO₄ at low temperatures. *Phys. Rev. Lett.* **82**, 628–631 (1999).
- Lanzara, A. *et al.* Evidence for ubiquitous strong electron-phonon coupling in high-temperature superconductors. *Nature* **412**, 510–514 (2001).
- Rossat-Mignod, J. *et al.* Neutron scattering study of the YBa₂Cu₃O_{6+x} system. *Physica C* **185–189**, 86–92 (1991).
- Norman, M. R. *et al.* Unusual dispersion and line shape of the superconducting state spectra of Bi₂Sr₂CaCu₂O_{8+ δ} . *Phys. Rev. Lett.* **79**, 3506–3509 (1997).

- Anderson, P. W. Is there glue in cuprate superconductors? *Science* **316**, 1705–1707 (2007).
- McMillan, W. L. & Rowell, J. M. Lead phonon spectrum calculated from superconducting density of states. *Phys. Rev. Lett.* **14**, 108–112 (1965).
- Lee, J. *et al.* Interplay of electron-lattice interactions and superconductivity in Bi₂Sr₂CaCu₂O_{8+ δ} . *Nature* **442**, 546–550 (2006).
- Wilson, S. D. *et al.* Resonance in the electron-doped high-transition-temperature superconductor Pr_{0.88}LaCe_{0.12}CuO_{4- δ} . *Nature* **442**, 59–62 (2006).
- d'Astuto, M. *et al.* Anomalous dispersion of longitudinal optical phonons in Nd_{1.86}Ce_{0.14}CuO_{4+ δ} determined by inelastic X-ray scattering. *Phys. Rev. Lett.* **88**, 167002 (2002).
- Pan, Z.-H. *et al.* Universal quasiparticle decoherence in hole- and electron-doped high-T_c cuprates. Preprint at (<http://www.arXiv.org/cond-mat/0610442>) (2006).
- Kashiwaya, S. *et al.* Tunneling spectroscopy of superconducting Nd_{1.85}Ce_{0.15}CuO_{4- δ} . *Phys. Rev. B* **57**, 8680–8686 (1998).
- Littlewood, P. B. & Varma, C. M. Anisotropic tunneling and resistivity in high-temperature superconductors. *Phys. Rev. B* **45**, 12636 (1992).
- Kirtley, J. R. & Scalapino, D. J. Inelastic-tunneling model for the linear conductance background in the high-T_c superconductors. *Phys. Rev. Lett.* **65**, 798–800 (1990).
- Matsui, H. *et al.* Direct observation of a nonmonotonic d_{x²-y²}-wave superconducting gap in the electron-doped high-T_c superconductor Pr_{0.89}LaCe_{0.11}CuO₄. *Phys. Rev. Lett.* **95**, 017003 (2005).
- Shan, L. *et al.* An universal law of the superconducting gap in the electron-doped cuprate superconductors. *Phys. Rev. B* (in the press). Preprint at (<http://www.arXiv.org/cond-mat/0703256>) (2007).
- Pilgram, S., Rice, T. M. & Sigrist, M. Role of inelastic tunneling through the insulating barrier in scanning-tunneling-microscope experiments on cuprate superconductors. *Phys. Rev. Lett.* **97**, 117003 (2006).
- Zhao, J. *et al.* Neutron-spin resonance in optimally electron-doped superconductor Nd_{1.85}Ce_{0.15}CuO₄. *Phys. Rev. Lett.* **99**, 017001 (2007).
- Zhu, J. X. *et al.* Fourier-transformed local density of states and tunneling into a d-wave superconductor with bosonic modes. *Phys. Rev. B* **73**, 014511 (2006).
- Lavrov, A. N. *et al.* Spin-flop transition and the anisotropic magnetoresistance of Pr_{1.3-x}La_{0.7}Ce_xCuO₄: Unexpectedly strong spin-charge coupling in the electron doped cuprates. *Phys. Rev. Lett.* **92**, 227003 (2004).
- Pintschovius, L. *et al.* Inelastic neutron scattering study of La₂CuO₄. *Prog. High Temp. Supercond.* **21**, 36–45 (1989).
- Renker, B. *et al.* Electron-phonon coupling in HTC superconductors evidenced by inelastic neutron scattering. *Physica B* **180**, 450–452 (1992).
- Pintschovius, L. & Reichardt, W. in *Physical Properties of High Temperature Superconductors* Vol. IV (ed. Ginsberg, D. M.) 295 (World Scientific, London, 1994).
- Crawford, M. K. *et al.* Infrared active phonons in (Pr_{2-x}Ce_x)CuO₄. *Solid State Commun.* **73**, 507–509 (1990).
- Homes, C. C. *et al.* Optical properties of Nd_{1.85}Ce_{0.15}CuO₄. *Phys. Rev. B* **56**, 5525–5534 (1997).
- Lynn, J. W. *et al.* Phonon density of states and superconductivity in Nd_{1.85}Ce_{0.15}CuO₄. *Phys. Rev. Lett.* **66**, 919–922 (1991).
- Persson, B. N. J. & Baratoff, A. Inelastic electron tunneling from a metal tip: the contribution from resonant processes. *Phys. Rev. Lett.* **59**, 339–342 (1987).
- Hwang, J., Timusk, T. & Carbotte, J. P. Scanning-tunneling spectra of cuprates. *Nature* **446**, E3–E4 (2007).
- Scalapino, D. J. Superconductivity: Pairing glue or inelastic tunnelling? *Nature Phys.* **2**, 593–594 (2006).
- Eliashberg, G. M. Interactions between electrons and lattice vibrations in a superconductor. *Sov. Phys. JETP* **11**, 696–702 (1960).

Supplementary Information is linked to the online version of the paper at www.nature.com/nature.

Acknowledgements We thank A. V. Balatsky, E. W. Hudson, P. Richard, G. Murthy, J. Engelbrecht and J. C. Davis for discussions and comments. This work was supported by the NSF and the DOE.

Author Information Reprints and permissions information is available at www.nature.com/reprints. Correspondence and requests for materials should be addressed to V.M. (madhavan@bc.edu).